

# Computational and Experimental Investigation of Flow and Convective Heat Transfer Along Rough Surfaces



C. Özman, T. Saner, F. Gül, M. Diederich, A. C. Benim, and U. Janoske

**Abstract** Flow and heat transfers along rough surfaces are investigated. A test facility is established, where rough surfaces generated by additive manufacturing can be tested. The computational work follows two goals. On the one hand, a computational tool is developed that can analyze the characteristics of a rough surface and generate rough surfaces with prescribed characteristics. On the other hand, Computational Fluid Dynamics (CFD) is applied for the analysis of flow and heat transfer along rough surfaces. The present focus is on the validation of turbulence models. Within this context, two alternative treatments, namely the wall functions (WF)-based approach and roughness resolving (RR) approach are assessed. Turbulence is modeled within a RANS (Reynolds Averaged Numerical Simulation) framework. All of the considered four turbulent viscosity models, using WF, showed a similar agreement with the measurements. Quantitatively, the realizable  $k$ - $\epsilon$  model is observed to deliver a better accuracy, in general, which is, then, also applied in RR calculations.

---

C. Özman · T. Saner · F. Gül · M. Diederich · A. C. Benim (✉)  
Center of Flow Simulation, Düsseldorf University of Applied Sciences, Düsseldorf, Germany  
e-mail: [alicemal@prof-benim.com](mailto:alicemal@prof-benim.com)

C. Özman  
e-mail: [cansu.oezman@hs-duesseldorf.de](mailto:cansu.oezman@hs-duesseldorf.de)

T. Saner  
e-mail: [taner.saner@hs-duesseldorf.de](mailto:taner.saner@hs-duesseldorf.de)

F. Gül  
e-mail: [fethi.guel@hs-duesseldorf.de](mailto:fethi.guel@hs-duesseldorf.de)

M. Diederich  
e-mail: [michael.diederich@hs-duesseldorf.de](mailto:michael.diederich@hs-duesseldorf.de)

U. Janoske  
Chair of Fluid Mechanics, Department of Mechanical Engineering, University of Wuppertal,  
Wuppertal, Germany  
e-mail: [janoske@uni-wuppertal.de](mailto:janoske@uni-wuppertal.de)

The RR approach showed a fair qualitative performance, which was, however, quantitatively not as good as the WF approach. This is attributed to the idealized geometry on the one hand and possible limitations on the RANS turbulence modeling approach on the other hand. The analysis will be deepened in the future work.

**Keywords** Fluid dynamics · Heat transfer · Surface roughness

## 1 Introduction

The additive manufacturing (AM) technology allows compact and lightweight heat exchangers to be produced, which are of importance in different areas, e.g. in aviation [1]. Surfaces generated by AM are, however, not smooth compared to conventional procedures, but exhibit roughness patterns, depending on the particular technique [2]. The main body of the existing knowledge in convective heat transfer [3] refers to smooth surfaces, while rough surfaces received comparably less attention. The purpose of the present research is to achieve a better understanding of forced convection along rough surfaces. Two roughness categories can be defined as (1) regular roughness, also called technical roughness or periodic roughness, where roughness elements consist of regular arrays of well-defined shapes such as pins and fins, and (2) irregular roughness, also called arbitrary or random roughness, where such regularities cannot be presumed.

In boundary layers, under certain conditions, the flows may be described by ordinary differential equations, employing boundary layer assumptions and similarity parameters [4, 5]. In most engineering applications, like the present one, this is prohibited by the prevailing flow conditions, geometry, and boundary conditions that necessitate the solution of the full Navier–Stokes equations [4]. Turbulent flows are characterized by extremely small time and length scales. Their direct numerical solution, the so-called Direct Numerical Simulation (DNS), is, thus, very expensive [6]. The common engineering approach is the solution of the time-averaged equations the so-called Reynolds Averaged Numerical Simulation (RANS) [6, 7]. The terms resulting from averaging are approximated using the so-called turbulence models [6]. Combinations of scale resolving and modeling approaches are the Unsteady RANS (URANS), Detached Eddy Simulation (DES), and Large Eddy Simulation (LES) [6, 8]. These turbulence modeling strategies were alternately applied in the previous studies on rough surfaces that are outlined below. The near-wall turbulence, with re-laminarization and its consequences on the mathematical modeling and discretization, requires special attention. An engineering approach is to approximate this flow by the so-called wall functions (WF) [6], derived under simplifying assumptions. For rough surfaces, the challenges in modeling the near-wall flow are increased, additionally, by the complex wall topology.

In modeling flow near rough walls, a straightforward approach is the full geometric resolution of the surface by the computational grid. In the case of regular roughness, the surface topology is easier to grasp. Turbulent flows over regular arrays of obstacles with well-defined shapes were presented by many researchers [9–12]. For irregular roughness, additional challenges exist due to the capturing and discretization of the surface topology. Numerical analysis of forced convection over irregularly rough surfaces was also presented by several authors, previously [13–16]. Obviously, the direct resolution of roughness is nearly impracticable for many engineering applications due to grid resolution requirements near walls. A remedy is provided by the WF modeling of near-wall turbulent flow [6], which allows an incorporation of the roughness effects through model constants. This is the main approach in engineering applications [21, 22]. A fundamental difficulty in using this approach is that the model is designed for sand grain roughness (SGR). For other roughness types, the model should be employed using an equivalent SGR. For this conversion, different procedures were proposed, including elaborate modifications of the WF [17–22]. However, given the large variety of roughness types, the proposed modifications are found not to be generally applicable with sufficient accuracy [23].

## 2 Experimental

A test system is constructed for the experimental part (Fig. 1). Arbitrary rough surfaces are produced by the SLS printing technique. The roughness is mapped by using a laser scanner. A high-power vacuum blower is used to manipulate the airflow. To obtain fully developed flow, a bell mouth and flow conditioner are used. Measurements are taken for different Reynolds numbers. The mass flow rate is measured by an orifice flow meter, cross-checking the results with a high-precision hot wire anemometer. The test section is uniformly heated with cartridge heaters. The pressure drop is measured between the inlet and outlet by a differential pressure transducer. RTD-type thermometers are placed in the channel as well as on the heated surface to obtain temperature measurements. The velocity profile in the boundary layer is measured with a specially designed hot wire anemometer (Dantec Dynamics, 55P15).

## 3 Surface Analysis and Reconstruction

A surface analysis program is created in the MATLAB environment [24]. For surface generation, a power spectrum density-based or autocorrelation-based concept can alternatively be used. The generated surface can then be written out as an STL file. The two concepts can also be used for the analysis of a measured surface.

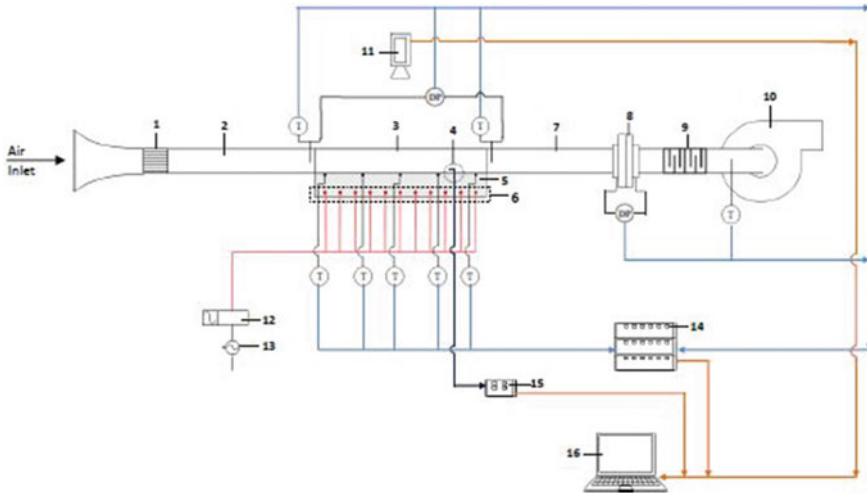


**Fig. 1** Test rig: T: thermocouple, DB: differential pressure transducer, 1: flow straightener, 2: entrance length, 3: test section, 4: hot wire anemometer, 5: aluminum block, 6: cartridge heaters, 7: calming length, 8: orifice plate and flanges, 9: mixing chamber, 10: high-pressure blower with frequency converter, 11: thermographic camera, 12: proportional control solid state relay, 13: power grid, 14: main data logger, 15: data logger of hot wire anemometer, and 16: computer

## 4 Mathematical and Numerical Flow Modeling

Incompressible flow with constant material properties described by Navier–Stokes equations is computationally modeled by the general-purpose CFD software ANSYS Fluent 18.0 [25], based on the Finite Volume Method. Lattice Boltzmann Method (LBM)-based procedures that may be more convenient in DNS analysis of the present problem are to be considered in the future work [26]. A coupled procedure is adopted for the solution of Navier–Stokes equations. For the discretization of the convective terms, the second-order accurate upwind scheme [25] is used for all variables. Within the scope of the current work, turbulence is modeled within the RANS framework, using different turbulent viscosity models [6, 25] including the Standard  $k$ - $\epsilon$  model (STD-KE) [6, 25], Renormalization Group Theory  $k$ - $\epsilon$  model (RNG-KE) [6, 25], Realizable  $k$ - $\epsilon$  model (REL-KE) [6, 25], and the Shear Stress Transport  $k$ - $\omega$  model (SST-KO) [6, 25] ( $k$ : turbulence kinetic energy;  $\epsilon$ : dissipation rate of  $k$ ;  $\omega$ : specific dissipation rate). DNS, LES, DES, and URANS studies are planned for the future. Flows in straight pipes and channels are considered. For the treatment of the near-wall flow, two approaches are applied: The wall function (WF) approach and the roughness resolving (RR) approach. The WF-based calculation is performed in 2D. The RR calculations are performed in 3D. In the RR calculations, the REL-KE is used as the turbulence model. In doing so, the so-called Enhanced Wall Treatment based

on Two-Layer Model [25, 27, 28] is employed to account for the re-laminarization effects. Due to space limitations, the governing equations of the models are not provided here, as they can be obtained through the cited sources. For convenience, a very basic discussion on WF and roughness modeling is presented below. Please note that, at the current stage, the WF model implemented in the used software [25] is used with its default settings.

#### **4.1 Roughness Modeling via Wall Functions: A Brief Overview**

For pressure gradient-free, unidirectional boundary layer flow along a straight wall, the time-averaged velocity ( $u$ ) as a function of distance from the wall ( $y$ ) can be described by a logarithmic function in the turbulent, near-wall region [3, 4]. A similar relationship can be derived for the time-averaged temperature ( $T$ ) utilizing the Reynolds analogy [3, 4]. This is the basis for the so-called “wall functions” (WF). They are normally expressed in terms of dimensionless quantities indicated by a “+” in the superscript, where the non-dimensionalization is done by the wall shear stress and material properties.

Experiments indicate that the effect of wall roughness can be expressed by a shift ( $\Delta B$ ) in the logarithmic law of the wall [4, 6, 25]

$$u^+ = \frac{1}{\kappa} \ln (E y^+) - \Delta B \quad (1)$$

where  $\kappa$  denotes the Von Karman constant [4] ( $\kappa = 0.41$ ), and  $E = 9.0$ . For tightly packed, uniform SGR, with a roughness height of  $k$ , analysis of experimental data reveals that the roughness effect can be classified into three categories in terms of dimensionless  $k$ : (1) hydrodynamically smooth, for  $k^+ \leq 2.25$ ; (2) transitional, for  $2.25 < k^+ < 90$ ; and (3) fully rough  $k^+ > 90$  [4]. In the first regime, the effect of roughness is neglected ( $\Delta B = 0$ ). For the remaining regimes, expressions of the form [29]

$$\Delta B = f(k^+) \quad (2)$$

are assumed. Presently, the empirical expressions from Cebeci and Bradshaw [29] are employed to relate  $\Delta B$  to  $k^+$ , which are based on Nikuradse’s SGR data [4].

## 5 Results

### 5.1 Validation of Turbulence Models for Wall Functions-Based Modeling

Turbulent fully developed pipe flow (diameter:  $D$ ) with SGR is calculated for different Reynolds numbers ( $Re = 5 \cdot 10^3, 1 \cdot 10^4, 2 \cdot 10^4, 3 \cdot 10^4, 4 \cdot 10^4, 5 \cdot 10^4, 7.5 \cdot 10^4, 1 \cdot 10^5, 2 \cdot 10^5, 5 \cdot 10^5, 1 \cdot 10^6$ ) and for different values of the relative roughness height ( $k/D = 0.001, 0.002, 0.004, 0.008, 0.016, 0.033$ ) using the above-mentioned turbulence models. The predictions are compared with the empirical data in terms of the friction factor ( $\lambda$ ) in Fig. 2.

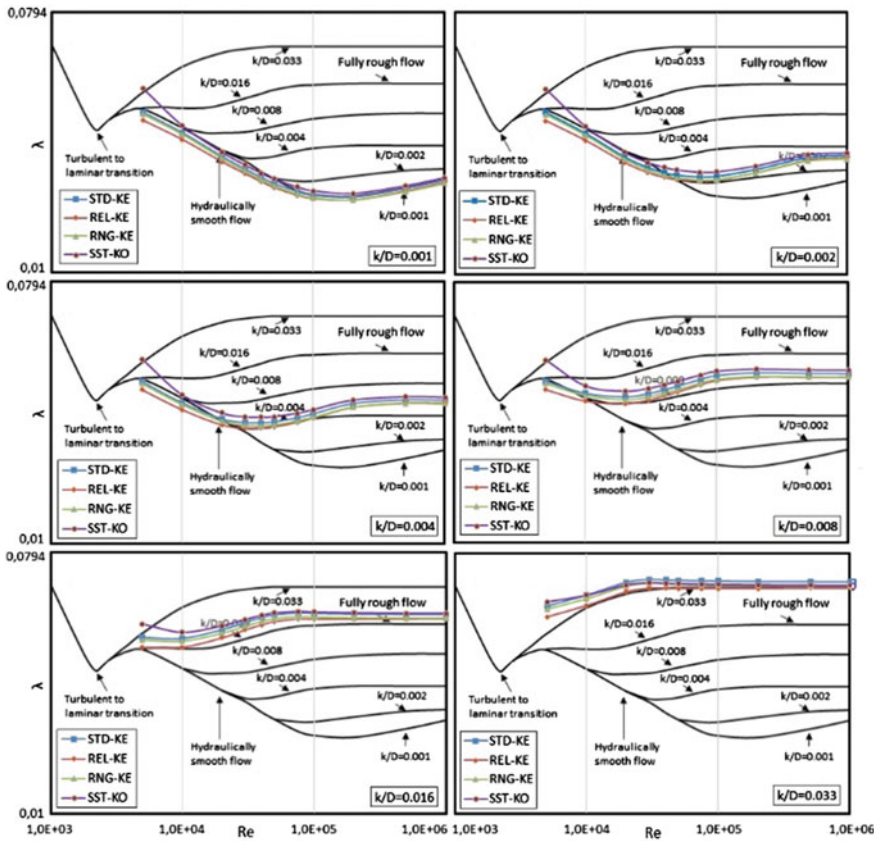


**Fig. 2** Predicted friction factors ( $\lambda$ ) as a function of Reynolds number ( $Re$ ) for different values of relative roughness ( $k/D$ ) for fully developed pipe flow, compared with empirical data (black lines, reproduced from Ref. [30])

In Fig. 2, one can see that all models show a fair qualitative agreement with the data, whereas quantitative differences exist. The differences between the models among one another are larger for low Re and get smaller with increasing Re. For low roughness ( $k/D \leq 0.004$ ), the models underpredict for low Re, and overpredict for high Re, except for SST-KO, which constantly overpredicts. For high roughness ( $k/D \geq 0.008$ ), all models overpredict for the whole Re range. Comparing the models with each other, a very clear distinction cannot be made. As a general trend, one can see that STD-KE and RNG-KE perform rather similar to each other, and SST-KO and REL-KE tend to have slightly higher and lower values, respectively. Overall, a better quantitative agreement of REL-KE with the measurements can be attested.

## 5.2 Validation of Roughness Resolving Approach Based on SGR

A reasonable first step toward the validation of a roughness resolving modeling approach can be the investigation of SGR, for which much data exists. This is attempted in the present study, as a basis. Most of the existing data on SGR is, however, for pipe flow. From a practical point of view, a planar channel flow is more amenable for a roughness resolving treatment. An engineering approach to utilize the pipe data for different channel shapes is provided by the concept of hydraulic diameter [3, 4]. Since this is an engineering approximation, its accuracy in converting the pipe data to a planar channel is analyzed first, for the presently considered case. For this purpose, the planar channel flow is calculated, and the results are compared with the pipe data, using the concept of hydraulic diameter. These calculations are performed for the relative roughness of  $k/D = 0.033$ , using the turbulence models REL-KE and SST-KO. The results obtained for  $Re = 5 \cdot 10^3, 1 \cdot 10^4, 2 \cdot 10^4, 3 \cdot 10^4, 4 \cdot 10^4$ , and  $5 \cdot 10^4$  are compared with pipe data in Fig. 3.

One can see in Fig. 3 that the deviation of the channel analogy to the pipe is larger for low Re and gets reduced for increasing Re. One can also observe that REL-KE-CHANNEL agrees better with the experiments, with quite good agreement for large Re.

In an attempt of obtaining a surface resolving solution for SGR, one shall first recognize that SGR represents, principally, an irregular roughness. In conceptual considerations, SGR is normally assumed to be represented by a tightly packed, regular array of perfect spheres with a uniform diameter ( $k$ ). It should be stated that this is a rather strong idealization of the reality. Not only because of the assumed perfect spherical shape, but also for the connection of the spheres to the wall. The spheres touch the wall at a point, leaving much free space in the next-to-wall region, which may not well correspond to reality. This is especially problematic for the thermal problem, since the roughness elements are thermally disconnected from the wall, as the ideal point contact allows no finite heat transfer area between the spheres



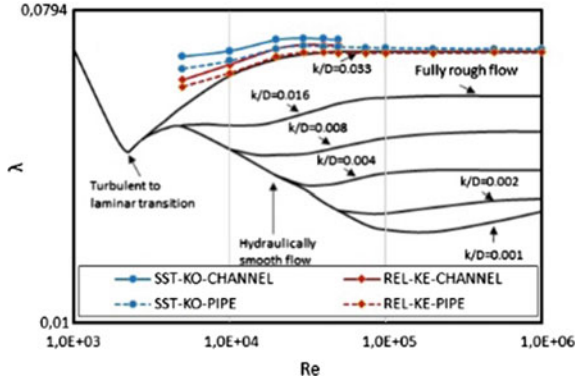


**Fig. 3** Predicted friction factors ( $\lambda$ ) as a function of Reynolds number ( $Re$ ) for  $k/D = 0.033$  obtained for fully developed pipe flow and fully developed channel with equivalent hydraulic diameter, compared with empirical data for pipe (black lines, reproduced from Ref. [30])

and the wall. Still, this idealization is applied for the sake of a systematic approach as a first step of the intended more detailed study.

In applying this idealization for SGR, inline and staggered arrangements of the spheres are considered to find out how much role the difference plays. The calculations are performed for four Reynolds numbers, i.e. for  $Re = 1 \cdot 10^4$ ,  $2 \cdot 10^4$ ,  $4 \cdot 10^4$ , and  $5 \cdot 10^4$ . Since REL-KE shows a more consistent behavior between pipe and channel, and a better agreement with the experiments, the REL-KE model is used in these calculations. Applying local grid adaptations, it is ensured that  $y^+$  values of the next-to-wall cells are everywhere well below unity. Detailed views of surface grids on the roughness elements are displayed in Fig. 4.

Detailed views of the predicted vector fields in a longitudinal plane near the wall, through the roughness elements, are displayed in Fig. 5, for inline and staggered arrangements of the roughness elements.

In Fig. 5, the recirculation zones with comparably low velocities within the spaces between the roughness elements can be observed, which also exhibit different patterns

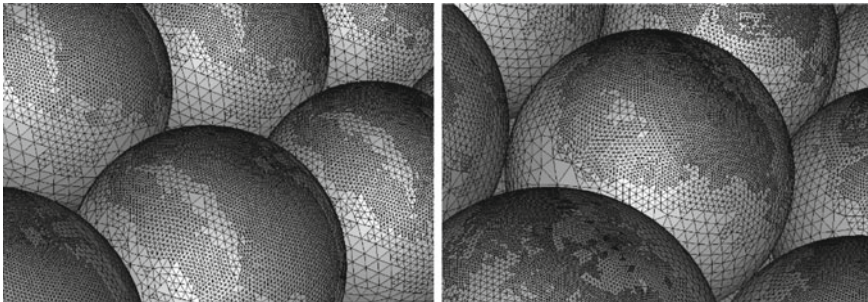


**Fig. 4** Surface grids on SGR elements. Left: inline arrangement, right: staggered arrangement



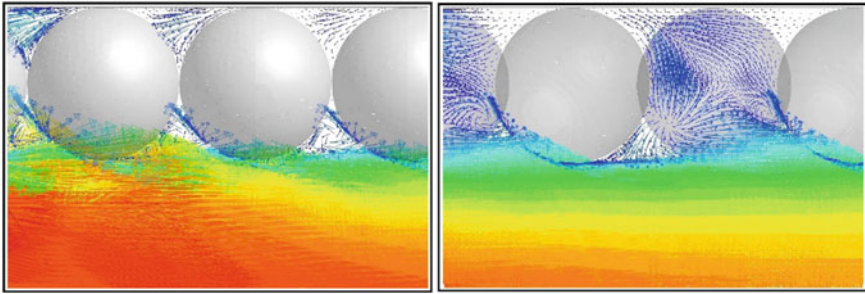


**Fig. 5** Detail velocity vectors near the wall in a longitudinal plane through roughness elements. Left: inline arrangement, right: staggered arrangement ( $k/D = 0.033$ ,  $Re = 50,000$ , REL-KE)

for the different arrangements of the roughness elements (a color scale is not provided, since it is about a qualitative discussion. Besides the vector length being proportional to the velocity magnitude, red and blue colors mark the maximum and minimum values of the velocity magnitude). One can see that the velocity starts to increase just above the roughness elements, which can, in a way, be interpreted as a kind of “lifting” of the boundary layer by the roughness elements. This can be seen to be in accordance with the empirically considered shift of the assumed boundary layer velocity profile as expressed in Eq. (1).

The thermal problem is posed as the heating of the fluid (air, Prandtl number = 0.7) by a hot wall. Isothermal boundary conditions are applied (Air inlet temperature: 25 °C, channel wall temperature: 50 °C). It is assumed that all solid surfaces including the planar wall and spheres have the same, constant wall temperature.

Detailed views of predicted temperature fields in a longitudinal plane near the wall through the roughness elements are displayed in Fig. 6, for both arrangements of the roughness elements. In the figure, the distribution of wall heat flux on the roughness elements is also displayed (a color scale is not provided, since it is about a qualitative discussion. Red and blue colors mark the maximum and minimum values of the corresponding variable). In the vicinity of the wall, up to a level of approx. mid-height of the roughness elements, the temperature distribution is quite uniform, which is the result of the mixing and homogenization caused by the recirculation zones. This, in return, seems to lead to comparably low local heat flux values, due to the prevailing low temperature difference. This can be observed on the wall-side surfaces of the spheres. On the flow side of the spheres, the roughness elements are subject to a unidirectional flow with high velocity, higher temperature gradients occur in the layers next to the roughness elements, and maximum heat flux values on the surfaces of roughness elements are observed here, on their upstream sides, due to the impingement effect.

Friction factors predicted by the surface resolving calculations are compared with the experiments in Fig. 7, where the wall functions-based solution is also indicated.

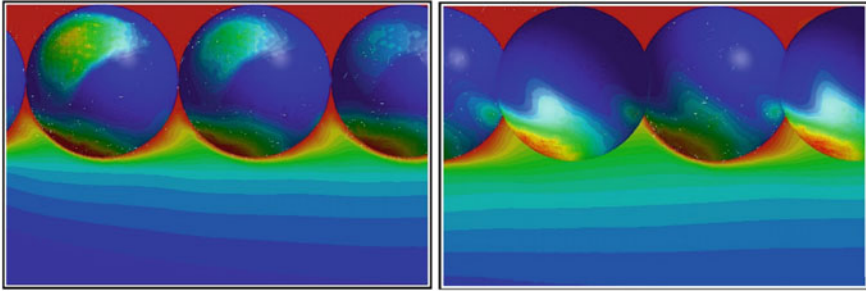


**Fig. 6** Detail temperature fields near the wall in a longitudinal plane through roughness elements, as well as wall heat flux distributions on the solid surfaces. Left: inline arrangement, right: staggered arrangement ( $k/D = 0.033$ ,  $Re = 50,000$ , REL-KE)

One can see that the RR calculations show a fair agreement with the measurements. This is, however, not as good as that of the WF approach, which is, however, empirically tuned to achieve the best accuracy exactly for SGR.

Predicted Nusselt numbers ( $Nu$ ) are compared with experimental values in Fig. 8. One can see that the results by the WF approach show a fairly good agreement with measurements. The  $Nu$  values obtained by the RR approach are, however, strongly overpredicting the experimental values.

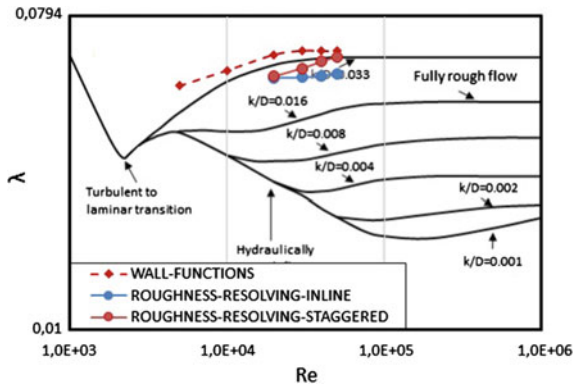


**Fig. 7** Predicted friction factors ( $\lambda$ ) as a function of Reynolds number ( $Re$ ) for SGR,  $k/D = 0.033$  obtained for fully developed pipe flow and fully developed channel flow with equivalent hydraulic diameter, compared with empirical data for pipe (black lines, reproduced from Ref. [30])

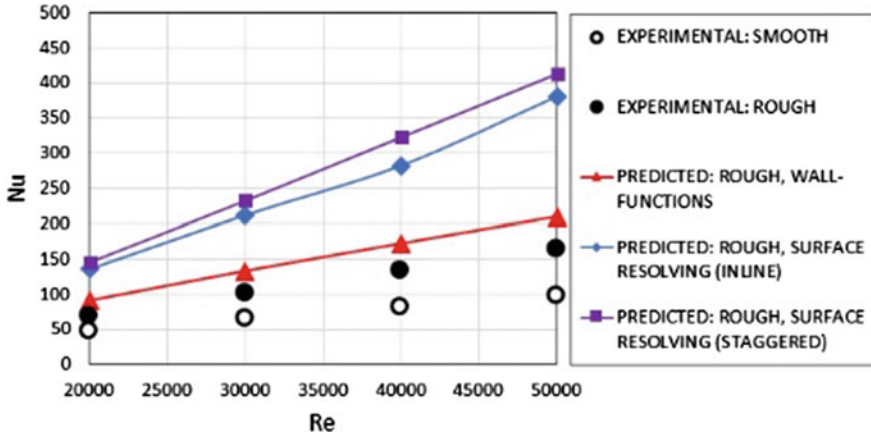


Fig. 8 Predicted and measured Nu as a function of Re for channel flow with SGR,  $k/D = 0.033$

### 5.3 Roughness Resolving Approach for Surface with Irregular Roughness

As the WF approach is tuned for SGR, the RR approach gains more value for non-SGR, irregular roughness patterns. In applying the RR approach, the discretization of a measured irregularly rough surface often represents a great challenge, due to very complex shapes on the rough surface.

An amenable approach is to re-construct the surface by keeping the main characteristics of the rough surface, but smoothing it, at the same time, at a certain level, by applying some kind of filtering to remove the too-spiky structures, to allow sufficient grid smoothness and stability.

Since this means some loss of topology information, it is a trade-off between accuracy and practicability, the optimal point of which is to be explored in the future studies.

Flow in a rectangular channel with an irregular surface roughness is considered for  $Re = 50,000$ . The generated computational surface grid for the measured, and subsequent to smoothing, re-constructed rough surface is displayed in Fig. 9.

The predicted distribution of wall shear stress in magnitude is presented in Fig. 10, where alternating changes between high and low values at the peaks and valleys can be observed (a color scale is not provided, since it is about a qualitative discussion. Red and blue colors mark the maximum and minimum values of the corresponding variable).

The calculated overall friction coefficient is observed to overpredict the measured value by about 20%, which may, at least partially, be caused by the smoothing applied to the surface.

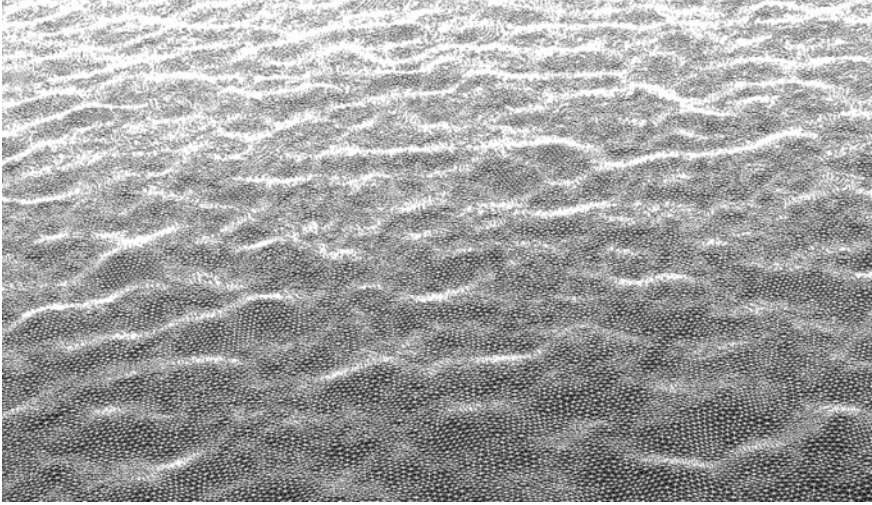


**Fig. 9** Surface grid for irregularly rough surface of channel flow

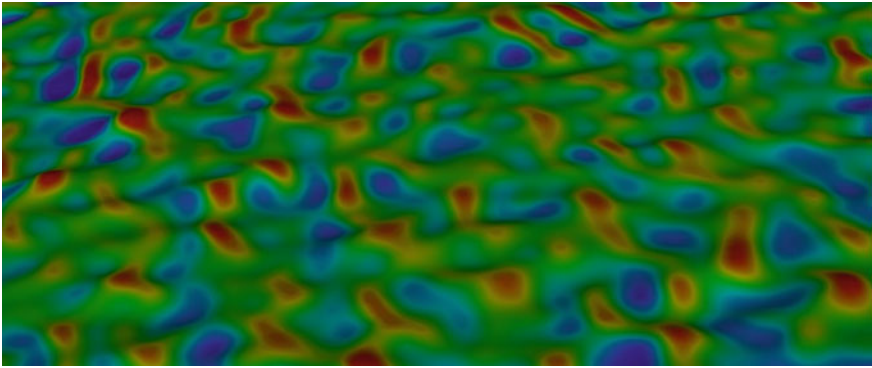


**Fig. 10** Distribution of wall shear stress magnitude on the rough surface

## 6 Conclusions

The WF-based roughness modeling is observed to provide a fair accuracy in the transitional region of pipe flow with SGR, where the realizable  $k-\epsilon$  turbulence model showed a slightly better quantitative accuracy compared to alternative two-equation models. Based on the measured SGR data in pipes and measurements performed in rectangular channels, the RR approach is observed to be less accurate in comparison. Improvements in the geometry representation and turbulence modeling are expected to lead to a better accuracy. This is to be explored in the future work.

**Acknowledgements** Funding by the Ministry for Economic Affairs, Innovation, Digitalization and Energy of the Government of the Federal State of North Rhine Westphalia (MWIDE NRW), Germany, is gratefully acknowledged [Project 005-2010-0082\_061]. Colleagues at ZIES (Centre Innovation Energy System, Prof. Adam) and ISAVE (Inst. Sound & Vibration Eng., Prof. Kameier) of the Düsseldorf University of Applied Science are gratefully acknowledged for their support in test rig installation and instrumentation.

## References

1. Gisario, A., Kazarian, M., Martina, F., Mehrpouya, M.: Metal additive manufacturing in the commercial aviation industry: a review. *J. Manuf. Syst.* **53**, 124–149 (2019)
2. Townsend, A., Senin, N., Blunt, L., Leach, R.K., Taylor, J.S.: Surface texture metrology for additive manufacturing: a review. *Precis. Eng.* **46**, 34–47 (2016)
3. Kays, W.M.: *Convective Heat and Mass Transfer*. McGraw-Hill, New York (2005)
4. Schlichting, H.: *Boundary Layer Theory*, 7th edn. McGraw-Hill, New York (1979)
5. Ali, R., Farooq, A., Shahzad, A., Benim, A. C., Iqbal, A., Razzaq, M.: Computational approach on three-dimensional flow of couple-stress fluid with convective boundary conditions. *Physica A* **553**, 124056 (2020)
6. Durbin, P.A., Petterson Reif, B.A.: *Statistical Theory and Modeling for Turbulent Flows*, 2nd edn. Wiley, Chichester (2011)
7. Benim, A.C., Cagan, M., Nahavandi, A., Pasqualotto, E.: RANS predictions of turbulent flow past a circular cylinder over the critical regime. In: *Proceedings of the 5th IASME/WSEAS International Conference on Fluid Mechanics and Aerodynamics*, pp. 232–237, Athens, Greece, August 25–27 (2007)
8. Benim, A.C., Nahavandi, A., Stopford, P.J., Syed, K.: URANS, LES and DES analysis of turbulent swirling flows in gas turbine combustors. *WSEAS Trans. Fluid Mech.* **1**(5), 465–472 (2006)
9. Xie, Z., Castro, I.P.: LES and RANS for turbulent flow over arrays of wall mounted obstacles. *Flow Turbul. Combust.* **91**, 291–312 (2006)
10. Ashrafian, A., Andersson, H.I.: Roughness effects in turbulent channel flow. *Progr. Comput. Fluid Dyn. Int. J.* **6**(1/2/3), 1–20 (2006)
11. MacDonald, M., Hutchins, N., Chung, D.: Roughness effects in turbulent forced convection. *J. Fluid Mech.* **861**, 138–162 (2019)
12. Benim, A. C., Diederich, M.: Prediction of roughness effects on wind turbine aerodynamics. In: *E3S Web of Conferences*, vol. 128, p. 09004 (2019)
13. Wang, Z. J., Chi, X., Shih, T., Bons, J.: Direct simulation of surface roughness effects with a RANS and DES approach on viscous adaptive Cartesian grids. In: *AIAA 2004-2420* (2004)
14. Yoon, S., Na, S., Wang, Z. J., Bons, J., Shih, T.: Flow and heat transfer over rough surfaces: usefulness of 2D roughness-resolved simulations. In: *AIAA 2006-0025* (2006)
15. Busse, A., Lützner, M., Sandham, N.D.: Direct numerical simulation of turbulent flow over a rough surface based on a surface scan. *Comput. Fluids* **116**, 129–147 (2015)
16. Foroghi, P., Strip, M., Frohnäpfel, B.: A systematic study of turbulent heat transfer over rough walls. *Int. J. Heat Mass Transf.* **127**, 1157–1168 (2018)
17. Coleman, H.W., Hodge, B.K., Taylor, R.P.: A re-evaluation of Schlichting's surface roughness experiment. *J. Fluids Eng.* **106**, 60–65 (1984)
18. Sigal, A., Danberg, J.E.: New correlation of roughness density effect on the turbulent boundary layer. *AIAA J.* **28**(3), 554–556 (1990)
19. Craft, T. J., Gerasimov, A. V., Iacovides, H., Launder, B. E.: Progress in the generalization of wall-function treatments. *Int. J. Heat Fluid Flow* **23**, 148–160 (2002)

20. Suga, K., Craft, T.J., Iacovides, H.: An analytical wall-function for turbulent flows and heat transfer over rough walls. *Int. J. Heat Fluid Flow* **27**, 852–866 (2006)
21. Ashrafian, A., Johansen, S. T.: Wall boundary conditions for rough walls. *Progr. Comput. Fluid Dyn. Int. J.* **7**(2/3/4), 230–236 (2007)
22. Chedevergne, F.: Analytical wall function including roughness corrections. *Int. J. Heat Fluid Flow* **73**, 258–269 (2018)
23. Diederich, M.: Modelling of turbulent flow over a surface with technical roughness. M.Sc. thesis, Department of Mechanical Process Engineering, Düsseldorf University of Applied Sciences (2018)
24. Saner, T.: Statistical analysis of 3D arbitrary surface roughness. M.Sc. thesis, Department of Mechanical and Process Engineering, Düsseldorf University of Applied Sciences (2021)
25. ANSYS Fluent 18.0, Theory Guide. [www.ansys.com](http://www.ansys.com)
26. Aslan, E., Taymaz, I., Benim, A. C.: Investigation of LBM curved boundary treatments for unsteady flows. *Eur. J. Mech. B/Fluids* **51**, 68–74 (2015)
27. Chen, H. C., Patel, V. C.: Near-wall turbulence models for complex flows including separation. *AIAA J.* **26**(6), 641–648 (1988)
28. Wolfshtein, M.: The velocity and temperature distribution of one-dimensional flow with turbulence augmentation and pressure gradient. *Int. J. Heat Mass Trans.* **12**, 301–318 (1969)
29. Cebeci, T., Bradshaw, P.: *Momentum Transfer in Boundary Layers*. Hemisphere, NY (1977)
30. Miller, D. S.: *Internal Flow Systems*, 2nd edn. British Hydromechanics Research Association (1990)